
Effect of Trapezoidal Geometry of Cross-Section of Annular Fin on Thermal Stresses and Strains

Ali Hatami^{†*}, Samira Payan[‡], & Mojtaba Hosseini^{††}

[†]Assistant Professor, Faculty of Mathematics, University of Sistan and Baluchestan, Zahedan, Iran.

[‡]Associate Professor, Faculty of Engineering (Shahid Nikbakht Engineering Faculty), Department of Mechanical Engineering, University of Sistan and Baluchestan, Zahedan, Iran

^{††}Ph.D. Student, Faculty of Mathematics, University of Sistan and Baluchestan, Zahedan, Iran.

*Email: ahatami@math.usb.ac.ir

ABSTRACT: Automotive chassis design, development is quite important in today's environment. This work is oriented towards analysis of a ladder chassis and space frame chassis design. The analysis of the designed models involves the use of three different materials. In this investigation two different conditions of vehicle loading are considered namely un-laden (without passengers that is the KERB weight of the vehicle) condition and the laden (with passengers and miscellaneous weight also called gross weight) condition. Analysis had resulted with various variables of stress indicating the stress levels minimum in unladen case as $3.00E-17$ and maximum in laden case as 29.8662, in case of space frame analysis the stress in minimum for steel with laden chassis as 0.001558 and maximum in case of composite material as 7.8447. These results would be useful with in selection of material for automotive frames.

KEYWORDS: Finite element method; Annular fin; Trapezoidal cross section; Thermal stress; Thermal strain.

INTRODUCTION

Fins are convenient engineering components for controlling heat transfer through a surface and have extensive application in several industries. The primary prerequisite for accurate prediction and proper control of fin's performance is a perfect knowledge about its mechanical response to expected and unexpected changes. As a result, in recent years many researchers have reported and modeled the performance of different fins under different conditions. Some of the previous works in this field are reviewed in the following.

In Mon and Gross [1] conducted a numerical study on the effects of the fin pitch on heat transfer, pressure drop and flow behavior in four rows of annular finned tubes in turbulent regimes. This study showed that the expansion of the boundary layer on the fin and tube surfaces mainly depends on the ratio of fin pitch to fin height. It was also reported that in linear arrangements, as the said ratio increases, the convective heat transfer coefficient increases and the pressure drop decreases. Bilerjen et al. [2] performed a similar analysis on a row of annular finned tubes in turbulent regimes with a more precise assessment of the effect of Reynolds number, fin pitch, fin height, fin thickness, and fin material on pressure drop and heat transfer. Their results showed that pressure drop and heat transfer is more influenced by fin thickness than by fin height and pitch. Another notable study on the effect of geometric variables on heat exchange is Shokouhmand et al. [3] where annular-finned tube was optimized using the principles of constructal theory to find the geometry that maximizes the heat transfer. This investigation showed that optimum geometry is a function of flow conditions. Another research on the optimization of geometry of annular-finned tube is Shokouhmand [4] which investigated the effect of geometric parameters including fin diameter, fin thickness, fin pitch, outer diameter of the tube, and physical parameters including the pressure drop number and Stanton. Kowsary and Farahani [5] also examined the heat transfer in annular fins made of orthotropic materials of various shapes and investigated the effects of the presence of a heat source, changes in convective heat transfer coefficient and non-uniform temperature of the fin base. Roy and Ghosal [6] presented a method for solving nonlinear differential equations for the analysis of steady-state heat transfer in annular fins and investigated the effects of variation of thermal conductivity with temperature on the efficiency of the fin and its temperature distribution. It is notable that because of high temperature difference between fin base and fin tip, determination of thermal stresses in fins is as important as determination of their temperature distribution. Some researchers have previously studied these stresses in thin annular fins. One of the most important of these researches is Yu and Chen

[7] where stresses and heat transfer of a one-dimensional annular fin were investigated in two cases with steady-state and transient conditions using a hybrid method. Chiu and Chen [8] studied the thermal stresses of an annular fin with temperature-dependent thermal conductivity. The results of this study showed that because of temperature-dependence of conductivity, even low temperature variations lead to significant variations in thermal stresses of annular fin. Wu [9] inverse Laplace transform and Simpson’s rule were used to investigate the transient thermal stress in a homogeneous and isotropic annular fin under the assumption that heat transfer is one-dimensional. In a study by Aksoy [10], the temperature distribution in an annular fin was obtained using the homotopy analysis method (HAM) and then compared with the results of finite difference numerical method. Hosseini et al. [11, 12] studied temperature and stress distribution fields inside a circular fin in laminar and turbulent flows using the liquid-solid-thermal coupling method. According to their results, the effective stress increased in the turbulent flow, but the worst location where the effective stress occurred was same as in the laminar flow. The tangential stress was not symmetrical in both laminar and turbulent flows, and the maximum absolute tangential stress was observed at the fin base in the frontal zone.

Other notable publications in this branch of literature include [13-18] which have investigated the temperature distribution in annular fins and also [19-22], which have studied the thermal stresses of these fins.

Fin geometry has a substantial impact on the temperature distribution and thereby thermal stresses, strains, and thermal efficiency of annular fins. As the above review of literature indicates, none of previous works in this field have investigated the impact of trapezoidal cross-section of an annular fin with gradual change in fin tip-to-base thickness ratio on thermal stress, strain, and efficiency. The present study examines this particular cross-section and investigates its effect on stress, strain, and thermal efficiency, and finally suggests geometry optimized with regard to these factors. In this study, fin base is assumed to have a fixed thickness of 0.004m, and fin tip thickness is gradually increased from 0.0005m to 0.008m. The results indicate that adjusting the fin tip so that it would be only slightly thick than fin base results in approximately the same strain distribution as rectangular cross section, reduced mean stress, and higher thermal efficiency, which leads to better heat transfer and thermal stress reduction.

PROBLEM DESCRIPTION AND GOVERNING EQUATIONS

Problem Description

This study considers a homogeneous and isotropic annular fin with base thickness of 0.004m and tip thickness varying from 0.0005m to 0.008m. Figure 1 illustrates the cross-section of this annular fin in three states. In this figure, w is the fin base thickness, w_{tip} is the fin tip thickness, r_b is the fin’s inner radius, and r_e is its outer radius. In the analysis of temperature distribution, the internal surface of the fin is assigned with the Constant-Temperature boundary condition and its upper, lower, and tip surfaces are assigned with Convective boundary conditions. The model is simulated three-dimensionally in ANSYS with the assumption of zero axial stress along the z-axis.

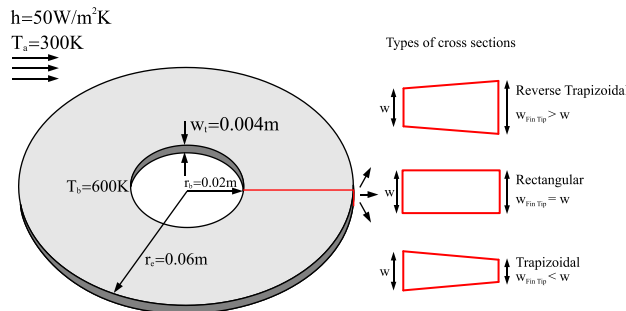


Figure 1. Images of annular fins with different cross sections

Governing Equations and Boundary Conditions

The governing equations comprise the energy equation, equilibrium equations, compatibility equations, and the constitutive equations of the material. The boundary conditions used for solving the energy equation are the Constant-Temperature at fin base and the Convective at fin’s upper, lower, and tip surfaces. The equilibrium, compatibility, and constitutive equations are solved with the assumption of zero radial stress at inner and outer radius and zero axial stress in the direction normal to the fin along the z-axis. Another important assumption of the problem is the separation of heat equations from stress, in the sense that, the energy equation is solved with the

thermal boundary conditions, and the resulting temperatures are then used to solve the equilibrium, compatibility and constitutive equations with the aforementioned stress boundary conditions.

A- Energy equation and boundary conditions

$$\begin{aligned}
 k\left(\frac{\partial^2 T}{\partial z^2} + \frac{1}{r} \frac{\partial}{\partial r} \left(\frac{\partial T}{\partial r}\right) + \frac{1}{r^2} \frac{\partial^2 T}{\partial \theta^2}\right) &= 0 \\
 T(r, \theta, z) &= T(r, \theta + 2\pi, z) \\
 T(r_b, \theta, z) &= 600k \\
 T(r_c, \theta, z) &= -\frac{k}{h} \frac{\partial T}{\partial r} \Big|_{r=r_c} + 300k \\
 T(r, \theta, 0) &= \frac{k}{h} \frac{\partial T}{\partial z} + 300k \\
 T(r, \theta, 0.004) &= -\frac{k}{h} \frac{\partial T}{\partial z} + 300k
 \end{aligned} \tag{1}$$

In Equations (1), T is the temperature of the fin and k is its thermal conductivity.

B- Equilibrium equations

In the absence of volume forces, the equilibrium equations are as follows.

$$\begin{aligned}
 \frac{\partial \sigma_r}{\partial r} + \frac{1}{r} \frac{\partial \tau_{r\theta}}{\partial \theta} + \frac{(\sigma_r - \sigma_\theta)}{r} &= 0 \\
 \frac{\partial \tau_{r\theta}}{\partial r} + \frac{1}{r} \frac{\partial \sigma_\theta}{\partial \theta} + \frac{2\tau_{r\theta}}{r} &= 0
 \end{aligned} \tag{2}$$

Where σ_r is the radial stress, σ_θ is the tangential stress, and $\tau_{r\theta}$ is the shear stress.

C-Compatibility equation

$$\frac{\partial^2 \varepsilon_r}{\partial \theta^2} + \frac{\partial^2 \varepsilon_\theta}{\partial r^2} = 2 \frac{\partial^2 \gamma_{r\theta}}{\partial r \partial \theta} \tag{3}$$

In Equation (3), ε_r is the radial strain, ε_θ is the tangential strain, $\gamma_{r\theta}$ is the shear strain.

C-Constitutive equation

$$\begin{aligned}
 \sigma_r &= \frac{E}{1-\nu^2} [\varepsilon_r + \nu \varepsilon_\theta - (1+\nu)\alpha^* \Delta T] \\
 \sigma_\theta &= \frac{E}{1-\nu^2} [\varepsilon_\theta + \nu \varepsilon_r - (1+\nu)\alpha^* \Delta T] \\
 \tau_{r\theta} &= \frac{E}{1+\nu} \varepsilon_{r\theta}
 \end{aligned} \tag{4}$$

In Equations (4), E is the modulus of elasticity, ν the Poisson's ratio, and α^* is the coefficient of thermal expansion.

D-Boundary conditions

$$\begin{aligned}
 (\sigma_r)_{r_b} &= 0, \quad (\sigma_r)_{r_e} = 0 \\
 r &= r_b, \quad v = 0, w = 0 \\
 r &= r_e, \quad v = 0 \\
 z &= 0, \quad v = 0 \\
 z &= 0.004, \quad v = 0
 \end{aligned}
 \tag{5}$$

In Equation (5), v and w are displacements.

As suggested in Chiu and Chen [7], S_{rr} and S_{θθ} are defined as follows.

$$S_{rr} = \frac{\sigma_r}{\alpha^* E} \tag{6}$$

$$S_{\theta\theta} = \frac{\sigma_\theta}{\alpha^* E} \tag{7}$$

In this study, the results are calculated for the fin with the following characteristics.

Table 1. Thermal, geometric, and material characteristics of the fin

Material properties	Fin dimensions	Specified temperatures
$\rho = 2700 \text{ kg / m}^3$	$\xi = r - r_b / r_e - r_b$	$T_a = 300 \text{ K}$
$E = 7.1 \times 10^{10} \text{ pa}$	$r_b = 0.02 \text{ m}$	$T_e = 300 \text{ K}$
$\nu = 0.33$	$r_e = 0.06 \text{ m}$	$T_b = 600 \text{ K}$
$c_p = 925 \text{ J / KgK}$	$w = 0.004 \text{ m}$	-
Tensile yield strength = 280MPa		-
Compressive yield strength = 280MPa		-

MESH INDEPENDENCE STUDY AND VALIDATION

In this study, mesh independence is checked for the mesh shown in Figure 2.

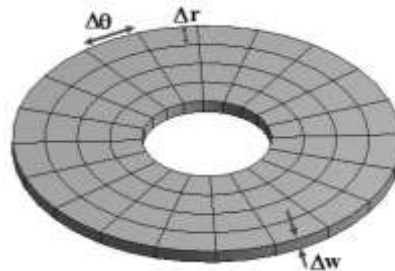


Figure 2. The studied mesh sizes

Mesh Independence

Figure 3 shows the variations of radial stress versus fin radius for different meshes. As shown in Figure 3, the radial stress curves obtained with Mesh No. 3 and 4 (Table 2) match each other with relative error of less than 1%. Therefore, subsequent analyses are performed with Mesh No. 4.

Table 2. Characteristic of the mesh sizes

Mesh No.	N – Δθ	N – Δr	N – Δw	Relative error
1	100	50	1	
2	200	100	1	1.8
3	400	200	1	0.8
4	800	400	1	0.01

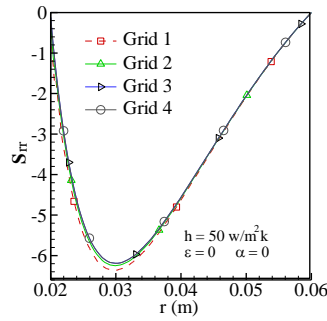


Figure 3. Variations of radial stress versus fin radius for different meshes

Validation

To validate the analysis, the results obtained for an annular fin with fixed thickness of 0.004 and temperature of 600 K (Figure 2), assigned at upper, lower, and tip surfaces with Convective and Radiation and Convection/Radiation boundary conditions are compared with the results reported in Ref.[5], [7] and [8]. As shown in Figure 4, the obtained radial stress matches the results of Chiu and Chen [7] with a relative error of 0.3%. As shown in Figure 5, the obtained tangential stress also matches those results, though with the maximum relative error of 5% in the fin base. This 5% error in the fin base can be attributed to the Fix boundary condition assigned to this position.

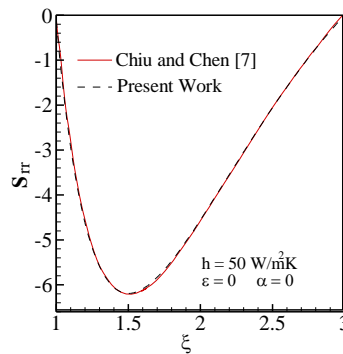


Figure 4. Comparison of radial stress obtained with Convective boundary condition with Ref.[7].

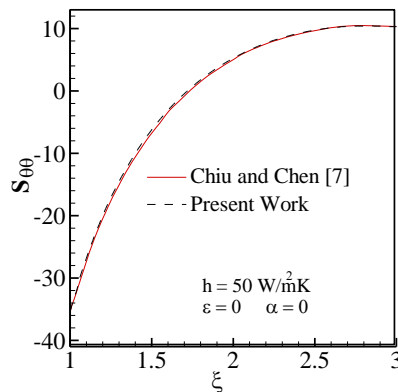


Figure 5. Comparison of tangential stress obtained with Convective boundary condition with Ref.[7]

In Tables 3, 4 and 5, the temperature distributions obtained in the present work are compared with the temperature distributions obtained for a similar annular fin but using different methods in [5, 7] and [8].

Table 3. Comparison of temperature values (in Kelvin) at specific intervals (with convective boundary condition assigned to the fin’s upper, lower, and tip surfaces)

Analysis method	$\xi = 0.25$	$\xi = 0.50$	$\xi = 0.75$	$\xi = 1.00$
-----------------	--------------	--------------	--------------	--------------

Reference [5]	577.826	565.053	558.482	556.513
Reference [7]	577.070	563.724	556.613	554.022
Reference [8]	576.990	563.880	556.860	554.310
Present work	576.980	563.900	556.860	554.330

Table 4. Comparison of temperature values (in Kelvin) at specific intervals (with convective boundary condition assigned to the fin’s upper and lower surfaces and insulated boundary condition assigned to fin tip)

Analysis method	$\xi = 1.00$	$\xi = 0.75$	$\xi = 0.50$	$\xi = 0.25$
Ref.[5]	558.30	560.19	566.28	578.52
Present work	558.36	560.19	566.35	578.45

Table 5. Comparison of temperature values (in Kelvin) at specific intervals (with radiation boundary condition assigned to the fin’s upper, lower, and tip surfaces)

Analysis method	$\xi = 1.00$	$\xi = 0.75$	$\xi = 0.50$	$\xi = 0.25$
Ref.[5]	584.895	585.566	587.798	592.181
Ref.[7]	582.652	583.636	586.323	591.342
Ref.[8]	582.630	583.620	586.290	591.270
Present work	582.730	583.700	586.360	591.310

Table 6. Comparison of temperature values (in Kelvin) at specific intervals (with convection/radiation boundary condition assigned to the fin’s upper, lower, and tip surfaces)

Analysis method	$\xi = 1.00$	$\xi = 0.75$	$\xi = 0.50$	$\xi = 0.25$
Ref.[5]	547.130	549.432	557.621	572.501
Ref.[7]	542.499	545.663	554.373	570.917
Ref.[8]	542.820	546.000	554.670	571.050
Present work	542.910	546.070	554.740	571.090

RESULTS AND DISCUSSION

In this section, we discuss the effect of the three cross sections shown in Figure (1) on tangential stress, radial stress, von Mises stress, radial strain, and thermal efficiency. The base of the fin is given a fixed temperature of 600 Kelvin and its upper, lower, and tip surfaces are assigned with convective boundary condition. The analyzed geometries can be categorized into 3 groups:

- 1- Geometries in which fin tip is as thick as fin base.
- 2- Geometries in which fin tip is thinner than fin base.
- 3- Geometries in which fin tip is thicker than fin base.

In all of above states, fin base has a fixed thickness of 0.004m; in the second group, fin tip thickness is gradually reduced from 0.004m to 0.005m; and in the third group, fin tip thickness is gradually increased from 0.004m to 0.008m by 0.001 steps.

Effect of Trapezoidal Geometry of the Annular Fin on Tangential and Radial Thermal Stresses

Effect of Thinner Fin Tip on Temperature Distribution and Tangential and Radial Stresses

The temperature distribution and tangential and radial stresses resulting from gradual thinning of fin tip are illustrated in Figures (6), (7) and (8). In Figure (6-b), the temperature distribution in the left side (the section before $r=0.03\text{m}$) is magnified. As can be seen, the temperature curve consists of 2 parts, and unlike the right side of the temperature curve, on the left side, in the areas near the fin base, thicker sections have lower temperatures.

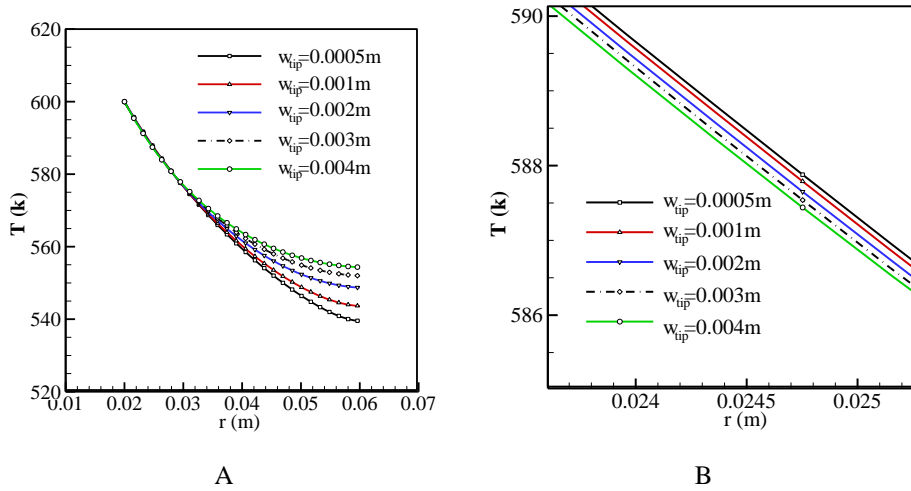


Figure 6. Temperature distribution in the annular fin with thinner tip; a) temperature distribution vs. radius from fin base to fin tip; b) magnified temperature distribution before $r=0.03\text{m}$.

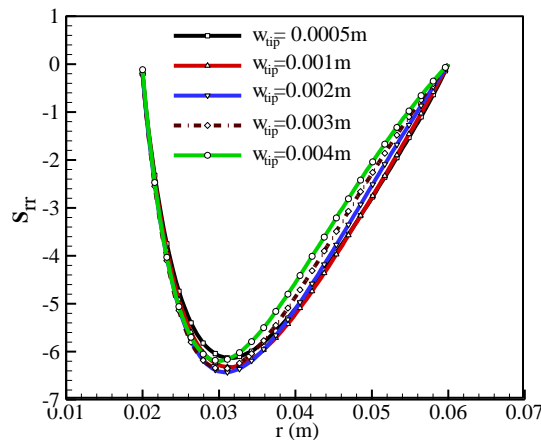


Figure 7. Radial stress vs. radius for thinner fin tips

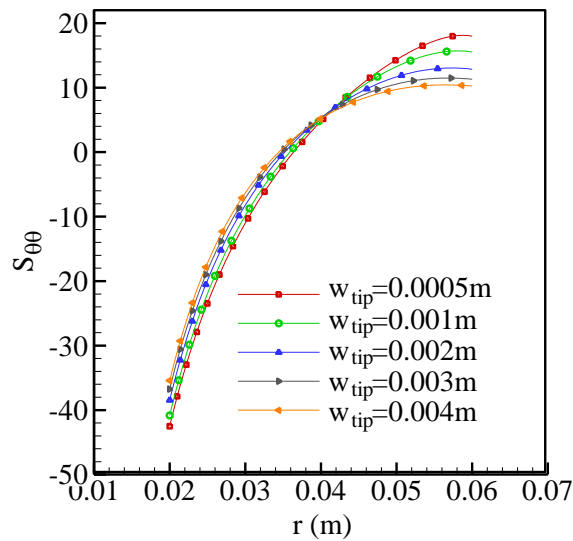


Figure 8. Tangential stress vs. radius for thinner fin tips

As could be predicted, because of the increase in the lateral surface area relative to the cross-sectional area, the decrease in fin tip thickness has led to higher temperature variations. Therefore, there appears to be a significant increase in radial stress as thickness decreases. This is clearly evident in the right side of the curve after the minimum point. But closer inspection of the temperature distribution reveals that for the radius of up to about $r=0.03\text{m}$, lower thicknesses correspond to lower temperatures. This has made the left side of the curves (near the fin base) and their minima unpredictable. As can be seen, the maximum compressive stress obtained with thinner tip is lower than those obtained with other geometries, but it only has a less than 1% difference from the rectangular cross-section. Table 7 shows the thermal efficiency given by Equation (8) for each cross section. It is notable that thinning the fin tip has led to 75% increase in tangential tensile stress at the fin tip.

$$\eta_f = \frac{q_f}{q_{\max}} = \frac{-kA_c \left. \frac{\partial T}{\partial r} \right|_{r=0.02\text{m}}}{hA_s(T_\infty - T_b)} \quad (8)$$

Effect of Thicker Fin Tip on Temperature Distribution and Tangential and Radial Stresses

Figures (9), (10) and (11) present the temperature distribution and tangential and radial stresses resulting from gradual thickening of fin tip. As shown in the temperature distribution diagram, using a fin tip that is thicker than its base leads to lower temperature variation in the fin, and thereby to reduced Tangential and Radial Stress. For instance, increasing the thickness of fin tip to 0.008m, results in approximately 10% reduction in maximum compressive stress.

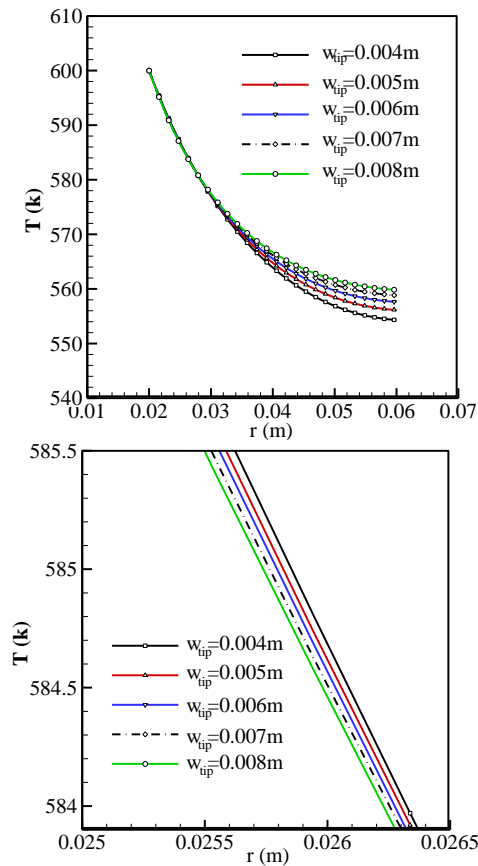


Figure 9. Temperature distribution in the annular fin with thicker tip; a) temperature distribution vs. radius from fin base to fin tip; b) magnified temperature distribution before $r=0.03\text{m}$

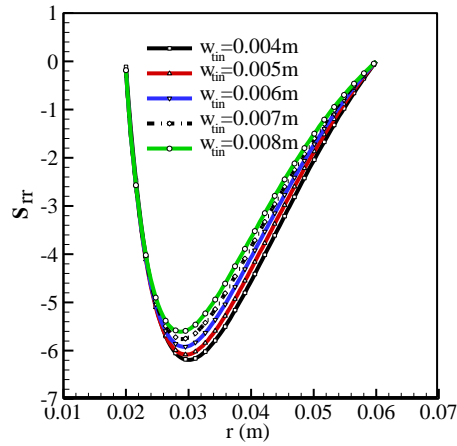


Figure 10. Radial stress vs. radius for thicker fin tips

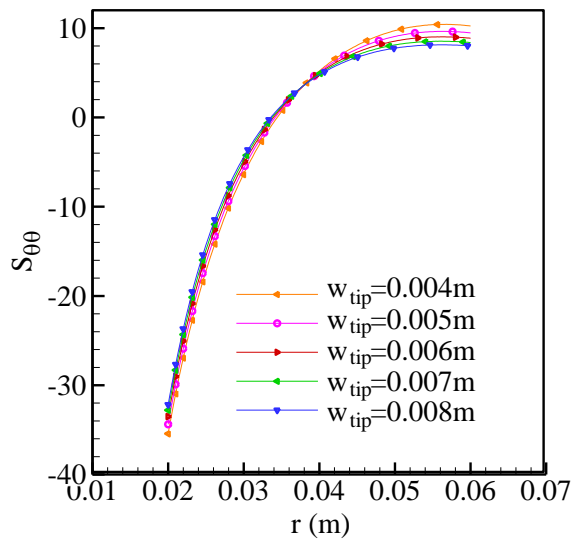


Figure 11. Tangential stress vs. radius for thicker fin tips

Table 7. Thermal efficiency of different geometries with varying fin tip thickness

η_f	q_{max} (W)	q_f (W)	A_s (m ²)	W_{tin} (m)
84.46	344.85	291.28	0.02299	0.008
84.42	339.45	286.58	0.02263	0.007
85.90	333.60	286.58	0.02224	0.006
85.65	329.10	281.88	0.02194	0.005
85.63	323.70	277.19	0.02158	0.004
85.68	318.00	272.49	0.02120	0.003
85.70	312.45	267.79	0.02083	0.002
85.72	306.90	263.09	0.02046	0.001
84.94	304.20	258.39	0.02028	0.0005

Effect Of Trapezoidal Geometry Of The Annular Fin On Von Mises Stress And Thermal Strain

Geometries must also be compared in terms of their effect on von Mises stress, as a representative of effective stress, and also on thermal strain and thermal efficiency. Naturally, von Mises stress at either end of the fin is a function of tangential stress. Equation (9) is used to determine the von Mises stress. As shown in Figure 12, increase in fin tip thickness results in a decrease in all strain values except in the inner radius.

$$\sigma_{von} = \sqrt{\sigma_r^2 + \sigma_{\theta\theta}^2 - \sigma_r \sigma_{\theta\theta}} \tag{9}$$

Also, tangential stress being greater than radial stress has led to alternatively positive and negative strains in the base and tip of fin respectively. In the area near the fin base, the fin is subjected to a dominant tangential compressive stress. This means that the element in this area are under pressure along the angle, and although they are under pressure along the radius as well (causing length reduction and negative strain), it is the tangential stress that plays the dominant role and the resulting compression along the angle causes a positive strain along the radial direction. The negative strain near the fin tip, which is greater than around the fin base, is caused by tangential and radial compressive stresses (both acting to reduce the length in this section). As can be seen, the lowest strain has been obtained with the maximum fin tip thickness (0.008 m).

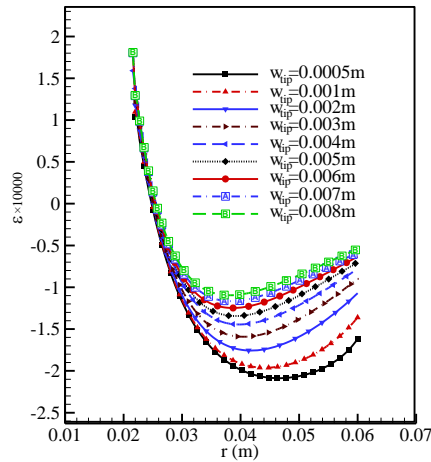


Figure 12. Strain diagram of annular fins of varying thicknesses

The von Mises stress diagram plotted in Figure 13 shows that increasing the fin tip thickness to 0.008m leads to 9.15% decrease in the von Mises stress at the fin base, and reducing this thickness to 0.0005m results in 20% increasing in stress from its maximum value. However, although the fin tip thickness of 0.0005m increases the maximum stress, it also sharply reduces the average stress on the right side of the curve in the range of $r=0.03\text{m}$ to $r=0.06\text{m}$.

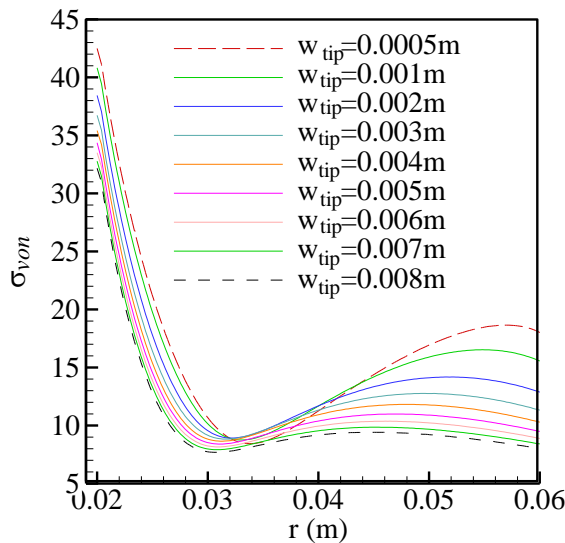


Figure 13. von Mises stress diagram for annular fins of varying thicknesses

CONCLUSION

Using the finite element method, the effect of the trapezoidal cross section of a circular fin on the stress, strain and thermal efficiency was analyzed. According to the results:

- a. As the trapezoidal cross section increased from to , the temperature difference between the fin base and tip decreased. Moreover, an increase in the cross section caused 9.15% reduction in the maximum von Mises stress at the fin base.

b. As the trapezoidal cross section decreased from to, the temperature difference between the fin base and tip increased.

Moreover, a decrease in the cross section caused 20% increase in the maximum von Mises stress.

According to the results, among different cases evaluated in this study, the fin with a tip thickness of 0.006 m was the best choice in the studied range. A relatively higher thermal efficiency was observed in this case, and the von Mises stress was lower by 5.38% than the rectangular fin.

Nomenclature

A_c	Cross sectional area, m^2
A_s	surface area, m^2
c_p	Specific heat at constant pressure, J/kgK
E	Modulus of elasticity, Pa
h	Convective heat transfer coefficient, W/m^2K
k	Thermal conductivity, W/mK
r	Radius, m
r_b	Inner radius of the fin, m
r_e	Outer radius of the fin, m
S_{rr}	Dimensionless radial stress
$S_{\theta\theta}$	Dimensionless tangential stress
T	Temperature, K
T_a	Fluid temperature, K
T_b	Temperature at fin base, K
u	Radial displacement, m
w	Fin base thickness, m
w_{tip}	Fin tip thickness, m
α	Surface absorptivity
β	Thermal expansion Coefficient
γ_r	Shear strain
ϵ	Surface emissivity
ϵ_r	Radial strain
ϵ_{θ}	Tangential strain
θ	Dimensionless temperature
ν	Poisson's ratio
ρ	Density, kg/m^3

REFERENCES

- [1] M.S., Mon, U. Gross, "Numerical study of fin-spacing effects in annular-finned tube heat exchangers". *International Journal of Heat and Mass Transfer*, vol. 47, pp. 1953-1964. 2004
- [2] H., Bilirgen, S., Dunbar, E.K. Levy, "Numerical modeling of finned heat exchangers". *Applied Thermal Engineering*, vol. 61, pp. 278-288. 2013
- [3] H., Shokouhmand, SH., Mahjoub, M. Salimpour, "Optimized architectural design of annular finned tube using the structure theory". *J. Modares Journal of Mechanical Engineering*, vol. 16, pp. 317-323. 2016
- [4] H. Shokouhmand, "Constructal design of finned tubes used in air-cooled heat exchangers". *Journal of Mechanical Science and Technology*, vol. 28, pp. 2385-2391. 2014
- [5] F., Kowsary, A. Farahani, "A numerical calculation of heat conduction in annular fins made of orthotropic materials". *Journal of the College of Engineering*, vol. 3, pp. 109-120. 1999
- [6] R., Roy, S. Ghosal, "Homotopy perturbation method for the analysis of heat transfer in an annular fin with temperature-dependent thermal conductivity", *Journal of Heat Transfer*, vol. 139, no. 2, pp. 022001. 2016

- [7] L. T., Yu, C. K. Chen, “Application of the hybrid method to the transient thermal stresses response in isotropic annular fins”. *Journal of Applied Mechanics-Transactions of The Asme*, vol. 66, pp. 340-346. 1999
- [8] C.H., Chiu, C.K. Chen, “Application of the decomposition method to thermal stresses in isotropic circular fins with temperature-dependent thermal conductivity”. *Acta Mechanica*, vol. 157, pp. 147–158. 2002
- [9] S. Wu, “Analysis on transient thermal stresses in an annular fin”. *Journal of thermal stresses*, vol. 20, pp. 591–615. 1997
- [10] I.G. Aksoy, “Thermal analysis of annular fins with temperature-dependent thermal properties”. *Applied Mathematics and Mechanics*, vol. 34, pp. 1349–1360. 2013
- [11] M., Hosseini, A., Hatami, S. Payan, “Impact of flow around annular fins on their thermal stresses and strains”. *Amirkabir Journal of Mechanical Engineering*, vol. 52, pp. 131-140, DOI:10.22060/MEJ.2018.14158.5811. 2018
- [12] M., Hosseini, A., Hatami, S. Payan, “Comparison of the effect of laminar and turbulent flow regimes on thermal stresses and strains in an annular fin”. *Journal of Mechanical Science and Technology*, vol. 34, pp. 413-424. 2020
- [13] H., Sen Peng, C.L. Chen, “Hybrid differential transformation and finite difference method to annular fin with temperature-dependent thermal conductivity”. *International Journal of Heat and Mass Transfer*, vol. 54, pp. 2427–2433. 2011
- [14] M.T., Darvishi, F., Khani, A. Aziz, “Numerical investigation for a hyperbolic annular fin with temperature dependent thermal conductivity”. *Propulsion and Power Research*, vol. 5, pp. 55-62. 2016
- [15] I.G. Aksoy, “Thermal analysis of annular fins with temperature-dependent thermal properties”. *Applied Mathematics and Mechanics*, vol. 34, no. 11, pp. 1349–1360. 2013
- [16] M. R., Hajmohammadi, E., Rasouli, M. Ahmadian Elmi, “Geometric optimization of a highly conductive insert intruding an annular fin”. *International Journal of Heat and Mass Transfer*, vol. 146, pp. 118910. 2020
- [17] H., Nemati, M., Moradaghay, S.A., Shekoochi, M. A. Moghimi, J. P. Meyer, “Natural convection heat transfer from horizontal annular finned tubes based on modified Rayleigh Number”. *International Communications in Heat and Mass Transfer*, vol. 110, pp. 104370. 2020
- [18] Y., Liu, X., Ma, X., Ye, Y., Chen, Y., Cheng, Z. Lan, “Heat transfer enhancement of annular finned tube exchanger using vortex generators: The effect of oriented functional circumferential arrangement”. *Thermal Science and Engineering Progress*, vol. 10, pp. 27-35. 2019
- [19] A., Mallick, R. Das, “Application of simplex search method for predicting unknown parameters in an annular fin subjected to thermal stresses”. *Journal of Thermal Stresses*, vol. 37, pp. 236-251. 2014
- [20] A., Mallick, D.K., Prasad, P.P. Behera, “Stresses in radiative annular fin under thermal loading and its inverse modeling using sine cosine algorithm (SCA)”. *Journal of Thermal Stresses*, vol. 42, no. 4, pp. 401-415. 2019
- [21] A., Yıldırım, D., Yarımabaç, K. Celebi, “Thermal stress analysis of functionally graded annular fin. *Journal of Thermal Stresses*, vol. 42, no. 4, pp. 440-451. 2019
- [22] M., Sudheer, G.V., Shanbhag, P., Kumar, S. Somayaji, “Finite element analysis of thermal characteristics of annular fins with different profiles”. *Journal of Engineering and Applied Sciences*, vol. 7, pp. 750-759. 2012